J. Chem. Eng. Data 1987, 32, 17-22

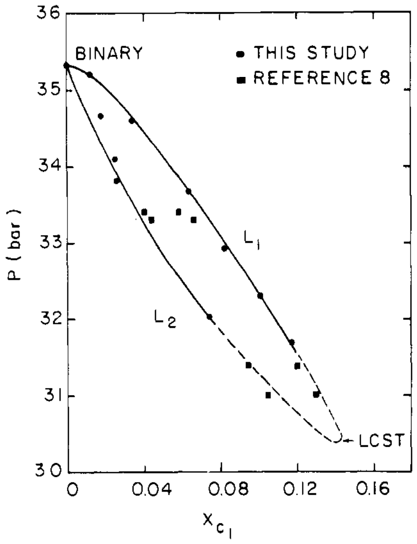

Figure 4. Comparison of L_1 and L_2 compositional data at 129 K for the system nitrogen + methane + ethane: methane mole fractions.

Glossary

K	the K point or upper critical end point of an L_1–L_2–V region, occurring when the L_2 phase becomes critically identical with the vapor phase V
L_1	liquid phase rich in solute (ethane or propane)
L_2	liquid phase lean in solute (ethane or propane)
LCST	lower critical solution temperature, occurring when the L_1 and L_2 phases become critically identical
Q	quadruple point, or four-phase point, herein an S–L_1–L_2–V point
S	solid phase
T	tricritical point, the intersection of an LCST and a K-point locus, whereby one has L_1=L_2=V criticality
V	vapor phase

Registry No. N_2, 7727-37-9; methane, 74-82-8; ethane, 74-84-0; propane, 74-98-6.

Literature Cited

(1) Hottovy, J. D.; Kohn, J. P.; Luks, K. D. *J. Chem. Eng. Data* **1981**, *26*, 1359
(2) Hottovy, J. D.; Kohn, J. P.; Luks, K. D. *J. Chem. Eng. Data* **1982**, *27*, 298.
(3) Merrill, R. C.; Kohn, J. P.; Luks, K. D. *J. Chem. Eng. Data* **1983**, *28*, 210.
(4) Merrill, R. C.; Luks, K. D.; Kohn, J. P. *J. Chem. Eng. Data* **1984**, *29*, 272.
(5) Merrill, R. C.; Luks, K. D.; Kohn, J. P. *Adv. Cryog. Eng.* **1984**, *29*, 949.
(6) Llave, F. M.; Luks, K. D.; Kohn, J. P. *Chem. Eng. Data* **1985**, *30*, 435.
(7) Chang, S. D.; Lu, B. C. Y. *Chem. Eng. Prog. Symp. Ser.* **1967**, *63*(81), 18.
(8) Yu, P.; Elshayal, I. M.; Lu, B. C. Y. *Can. J. Chem. Eng.* **1969**, *47*, 495.
(9) Gasem, K. A. M.; Hiza, M. J.; Kidnay, A. J. *Fluid Phase Equilib.* **1981**, *6*, 181.
(10) Poon, D. P. L.; Lu, B. C. Y. *Adv. Cryog. Eng.* **1974**, *19*, 292.
(11) Kremer, H.; Knapp, H. *Hydrocarbon Process.* **1983**, *62*(4), 79.
(12) Stroud, L.; Devaney, W. E.; Miller, J. E. *Soc. Pet. Eng. J.* **1961**, *1*, 137.
(13) Luks, K. D.; Kohn, J. P. *Proc. 63rd Annu. GPA Conv.* **19848** *181*.
(14) Kidnay, A. J.; Miller, R. C.; Parrish, W. R.; Hiza, M. J. *Cryogenics* **1975**, *15*, 531.
(15) Graboski, M. S.; Daubert, T. E. *Ind. Eng. Chem. Process Des. Dev.* **1978**, *17*, 443.
(16) Graboski, M. S.; Daubert, T. E. *Ind. Eng. Chem. Process Des. Dev.* **1978**, *17*, 448.

Received for review June 3, 1985. Accepted July 29, 1986. We are grateful for the support of this work provided by the Gas Processors Association (Research Project 795), Tulsa, OK. The apparatus was assembled under research grants from the National Science Foundation.

Excess Gibbs Energies and Excess Volumes of Some Alcohol–Methyl Ester Binary Mixtures

Josefa Fernández,[†] Charles Berro,* and André Péneloux

Laboratoire de Chimie-Physique, Faculté des Sciences de Luminy, 13288 Marseille Cedex 9, France

Isothermal vapor–liquid equilibrium data for the mixtures 1-butanol–methyl propanoate and 1-butanol–methyl butanoate have been measured by using a recirculating still. The excess molar volumes of the same mixtures and those of the system 1-pentanol–methyl butanoate were obtained from measurements of the density with an Anton Paar densimeter. The vapor–liquid equilibrium data were reduced according to the maximum likelihood principle. The parameters of the NRTL, Wilson, and UNIQUAC equations were calculated.

Introduction

This paper can be considered as a continuation of our previous studies on the excess thermodynamic properties of the binary systems formed by methyl ester and alcohol (*1*, *2*). In the present paper we report the results of vapor–liquid equilibrium measurements for the system 1-butanol–methyl propanoate at 348.15 K and for 1-butanol–methyl butanoate at 348.15 and 368.19 K. We also report the excess volume measurements at 298.15 and 308.15 K for the former system and at 298.15 K for the latter. The excess volumes of the system 1-pentanol–methyl butanoate at 298.15 K are also presented.

Experimental Section

Materials. The 1-butanol and 1-pentanol employed were Merck "zur analyse" products with a stated minimum purity of 99.5% and 99%, respectively. The esters were supplied by Fluka with a purity of 99%. The reagents were purified by distillation at atmospheric pressure, in a 60 real plate Oldershaw column. In Table I, we compare the measured densities and vapor pressures of the purified products with the literature values.

Apparatus and Procedure. Vapor–liquid equilibrium data were determined at constant temperature by using a still de-

---

[†] Current address: Departamento de Física Fundamental, Facultad de Física, Universidad de Santiago, Santiago de Compostela, Spain.

0021-9568/87/1732-0017$01.50/0

Table I. Physical Properties of Pure Components

	density(298.15)/(g cm^{-3})		vapor press., kPa			
			348.15 K		368.19 K	
compound	this work	lit.	this work	lit.	this work	lit.
1-butanol	0.805 75	0.805 75[a]	17.208	17.208[d]	42.367	42.362[d]
1-pentanol	0.810 86	0.810 80[a]				
methyl propanoate	0.909 17	0.909 32[b] 0.908 90[c]	86.907	86.436[e] 87.737[f]		
methyl butanoate	0.892 48	0.892 60[b]	40.075	40.040[g]	79.671	79.639[g]

[a] Reference *15*. [b] Reference *16*. [c] Reference *12*. [d] Reference *17*. [e] Reference *18*. [f] Reference *19*. [g] Reference *20*.

Table II. Experimental Excess Volume Data

temp/K	x_1^0	$v^{E0}/(cm^3\ mol^{-1})$	temp/K	x_1^0	$v^{E0}/(cm^3\ mol^{-1})$	temp/K	x_1^0	$v^{E0}/(cm^3\ mol^{-1})$
1-Butanol (1)–Methyl Propanoate (2)				0.4432	0.293		0.6906	0.187
298.15	0.0445	0.052		0.5177	0.296		0.7456	0.166
	0.1051	0.112		0.5615	0.291		0.7837	0.151
	0.1584	0.151		0.5911	0.289		0.7939	0.148
	0.1808	0.174		0.6102	0.283		0.8107	0.138
	0.2138	0.185		0.6225	0.280		0.8702	0.106
	0.2661	0.210		0.6786	0.266		0.9119	0.077
	0.3032	0.230		0.6837	0.261		0.9277	0.065
	0.3426	0.240		0.7472	0.230		0.9718	0.029
	0.3429	0.247		0.7829	0.211			
	0.3670	0.249		0.8360	0.176	1-Pentanol (1)–Methyl Butanoate (2)		
	0.4300	0.258		0.8881	0.133	298.15	0.0469	0.058
	0.5042	0.261		0.9150	0.108		0.1042	0.112
	0.5303	0.261		0.9469	0.083		0.1495	0.140
	0.5798	0.258		0.9510	0.069		0.1881	0.165
	0.6252	0.246					0.2304	0.188
	0.6812	0.229	1-Butanol (1)–Methyl Butanoate (2)				0.2733	0.205
	0.7228	0.215	298.15	0.0390	0.043		0.3104	0.219
	0.7703	0.193		0.0955	0.089		0.3676	0.239
	0.7784	0.183		0.1182	0.105		0.4132	0.244
	0.7963	0.173		0.1692	0.136		0.4753	0.251
	0.8796	0.123		0.2353	0.168		0.5044	0.252
	0.8978	0.105		0.2503	0.172		0.5407	0.252
	0.9524	0.055		0.3313	0.198		0.5786	0.246
308.15	0.0460	0.063		0.3591	0.204		0.6558	0.231
	0.1039	0.126		0.3933	0.212		0.6625	0.227
	0.1604	0.176		0.4496	0.215		0.7071	0.211
	0.2060	0.209		0.4783	0.216		0.7509	0.192
	0.2462	0.230		0.5313	0.213		0.7983	0.167
	0.2917	0.254		0.5685	0.212		0.8456	0.137
	0.3613	0.278		0.6067	0.205		0.8932	0.103
	0.4087	0.288		0.6307	0.203		0.9563	0.046

Table III. Excess Volumes, Parameters of Eq 1, and Values of the Standard Deviation in v^E

	1-butanol (1)–methyl propanoate (2)		1-butanol (1)–methyl butanoate (298.15 K)	1-pentanol (1)–methyl butanoate (298.15 K)
	298.15 K	308.15 K		
$A_j \pm \sigma/(A_j)/(cm^3\ mol^{-1})$	1.04802 ± 0.00444	1.18888 ± 0.00483	0.86215 ± 0.00211	1.01113 ± 0.00265
	−0.03145 ± 0.00817	−0.02430 ± 0.01546	−0.04269 ± 0.00424	0.01217 ± 0.00884
	0.17308 ± 0.02016	0.11269 ± 0.05077	0.18551 ± 0.00949	0.03031 ± 0.02780
		0.04723 ± 0.03972		−0.12118 ± 0.02365
		0.28631 ± 0.08437		0.25344 ± 0.04916
$\sigma(\rho)/(g\ cm^{-3})$	0.00003	0.00002	0.00001	0.00001
$\sigma(\rho)/(cm^3\ mol^{-1})$	0.003	0.003	0.001	0.001

signed by Berro et al. (*3*). The temperature of the equilibrium cell was measured with a LAUDA R42 digital thermometer with a platinum sensor which has a precision of 0.01 K. The pressure was measured by means of a Texas Instruments precision pressure gauge with a fused-quartz Bourdon tube. The inaccuracy of the pressure measurements was determined to be $\sigma_e(P)$ = 0.009 kPa in agreement with the calibration chart and the specifications of the apparatus. Samples of the liquid and condensed vapor were withdrawn from the ebulliometer through a silicon rubber septum by using a gas-tight syringe. The composition of each phase was determined by densimetric analysis using an Anton Paar DMA 60 vibrating-tube densimeter equipped with a DMA 601 M cell. The cell temperature was measured by the LAUDA R42 digital thermometer with another platinum sensor.

The excess volumes were previously determined in the same densimeter. Binary mixtures were prepared by weighing, using a technique designed by Berro and Pêneloux (*4*) to prevent their partial evaporation.

Experimental Results and Treatment of Data

Excess Volumes. Table II shows the excess volumes obtained from density data for the mixtures studied. In each case, a variable-degree Redlich–Kister polynomial of the form

$$v^E/(x_1x_2) = \sum_{j=1}^{m} A_j(x_1 - x_2)^{j-1} \qquad (1)$$

was fitted to the v^{E0} data. Here x_1 is the mole fraction of alcohol.

Table IV. Experimental Vapor–Liquid Equilibrium Data for the System 1-Butanol (1)–Methyl Propanoate (2) at 348.15 K

x_1^0	y_1^0	P^0/kPa	$\ln \gamma_1^0$	$\ln \gamma_2^0$
0.0713	0.0283	83.181	0.6113	0.0033
0.1120	0.0432	81.013	0.5572	0.0073
0.1572	0.0590	78.748	0.5026	0.0156
0.2002	0.0727	76.608	0.4431	0.0269
0.2504	0.0900	74.160	0.4015	0.0416
0.3058	0.1069	71.315	0.3361	0.0620
0.3605	0.1234	68.641	0.2783	0.0885
0.3930	0.1348	66.948	0.2563	0.1035
0.4822	0.1628	62.392	0.1726	0.1613
0.5203	0.1787	60.192	0.1551	0.1838
0.5463	0.1898	58.787	0.1438	0.2030
0.6098	0.2174	54.846	0.1025	0.2518
0.6480	0.2372	52.301	0.0830	0.2830
0.6897	0.2629	49.369	0.0675	0.3186
0.7298	0.2911	46.368	0.0521	0.3568
0.7833	0.3367	42.084	0.0326	0.4163
0.8255	0.3865	38.107	0.0213	0.4577
0.8654	0.4492	34.088	0.0156	0.5002
0.9386	0.6369	25.618	0.0037	0.5876
0.9666	0.7607	21.985	0.0016	0.6288

Table V. Experimental Vapor–Liquid Equilibrium Data for the System 1-Butanol (1)–Methyl Butanoate (2)

x_1^0	y_1^0	P^0/kPa	$\ln \gamma_1^0$	$\ln \gamma_2^0$
		348.15 K		
0.0770	0.0621	39.519	0.6049	0.0024
0.1170	0.0899	39.182	0.5477	0.0083
0.1625	0.1198	38.754	0.4952	0.0172
0.2073	0.1467	38.265	0.4415	0.0288
0.2473	0.1694	37.805	0.3969	0.0418
0.3028	0.2000	37.104	0.3418	0.0627
0.3816	0.2413	36.030	0.2692	0.1011
0.4254	0.2642	35.344	0.2322	0.1252
0.4657	0.2869	34.686	0.2055	0.1483
0.4993	0.3032	34.142	0.1756	0.1747
0.5222	0.3173	33.725	0.1641	0.1891
0.5582	0.3382	33.032	0.1407	0.2161
0.5830	0.3521	32.520	0.1222	0.2374
0.6104	0.3726	31.931	0.1148	0.2554
0.6451	0.3963	31.115	0.0957	0.2849
0.7214	0.4566	29.111	0.0601	0.3567
0.8205	0.5627	25.930	0.0265	0.4659
0.8660	0.6285	24.190	0.0148	0.5271
0.9042	0.7016	22.442	0.0079	0.5700
0.9623	0.8540	19.497	0.0036	0.6496
		368.19 K		
0.0515	0.0450	79.461	0.4798	0.0043
0.1496	0.1225	78.508	0.4021	0.0174
0.1903	0.1515	77.863	0.3657	0.0250
0.2343	0.1817	77.088	0.3295	0.0351
0.2706	0.2038	76.416	0.2915	0.0479
0.3070	0.2290	75.643	0.2718	0.0573
0.3862	0.2793	73.807	0.2167	0.0877
0.4219	0.3013	72.846	0.1913	0.1041
0.4511	0.3194	72.046	0.1719	0.1191
0.4963	0.3492	70.662	0.1467	0.1417
0.5611	0.3946	68.398	0.1145	0.1760
0.6087	0.4311	66.641	0.0962	0.2036
0.6496	0.4606	65.018	0.0733	0.2371
0.7359	0.5410	61.101	0.0490	0.2987
0.7900	0.5974	58.218	0.0302	0.3503
0.8339	0.6535	55.542	0.0201	0.3894
0.8952	0.7488	51.417	0.0102	0.4537
0.9282	0.8143	48.803	0.0070	0.4793
0.9650	0.8970	45.721	0.0012	0.5453

The parameters A_j of eq 1 are given in Table III with the values of root mean square deviations of the excess volumes and densities

$$\sigma(v^E) = \{\sum_{i=1}^{N}[v_i^{E0} - v^E(x_{1i}^0, A)]^2/(N - m)\}^{1/2} \qquad (2)$$

Table VI. Results of Vapor–Liquid Equilibrium Data Reduction

	1-butanol–methyl propanoate at 348.15 K	1-butanol–methyl butanoate	
		348.15 K	368.19 K
$A_j \pm \sigma(A_j)$	0.67396 ± 0.00056 −0.00193 ± 0.00032	0.69761 ± 0.00050 0.00173 ± 0.00031	0.56917 ± 0.00054 −0.00325 ± 0.00035 −0.00582 ± 0.00034
$\sigma_e(\rho)/(\text{g cm}^{-3})$	0.00007	0.00005	0.00007
$\sigma_e(x_1)$	0.00065	0.00060	0.00065
$\sigma_e(T)/\text{K}$	0.01	0.02	0.02
$\sigma_e(P)/\text{kPa}$	0.009	0.009	0.009
WRMSD	1.43	1.86	1.61

where N is the number of experimental values v_i^{E0} and m is the number of parameters. $\sigma(\rho)$ was calculated in a similar way.

Vapor–Liquid Equilibrium Data. In Tables IV and V we present isothermal vapor–liquid equilibrium data together with the values of the liquid-phase activity coefficients calculated according to the expression

$$\gamma_i^0 = \frac{p^0 y_i^0}{p_i^s x_i^0} \times \exp\left[\frac{(v_i - B_{ii})(P_i^s - P^0) + \delta_{12}(1 - y_i^0)^2 P^0}{RT}\right], \quad i = 1, 2 \qquad (3)$$

where $\delta_{12} = 2B_{12} - B_{11} - B_{22}$ and P^0, x_i^0, and y_i^0 are the experimental values of pressure, liquid mole fractions, and vapor mole fractions, respectively. B_{11}, B_{22}, and B_{12} are the virial coefficients calculated by the method of Hayden and O'Connell (*5*); v_i and P_i^s are the liquid molar volume and the measured vapor pressure of pure ith component, respectively.

We have applied to our VLE data the observed deviation reduction method proposed by Neau and Pêneloux (*6*). This method permits the simultaneous estimation of the fitting parameters and the experimental inaccuracies. In this method the excess Gibbs energies are fitted to a Redlich–Kister polynomial of the form

$$g^E/(RTx_1x_2) = \sum_{j=1}^{m} A_j Y_j$$

$$Y_j = (2j - 1)(2x_1 - 1)^{j-1} \qquad (4)$$

where x_1 is the mole fraction of 1-butanol and m is the number of A_j parameters. This number is not fixed in advance but is chosen during the reduction procedure as the lowest degree allowing the avoidance of systematic deviations arising from the model.

The A_j parameters and the experimental inaccuracies have been obtained by applying the maximum likelihood principle to the objective function S (see Appendix A). Furthermore, the thermodynamic consistency of the measured VLE data was checked by using the weighted root mean square deviation (WRMSD), defined as

$$\text{WRMSD} = \left[\frac{S}{2N - m}\right]^{1/2} \qquad (5)$$

If there are no systematic deviations and if the experimental inaccuracies have been correctly estimated, the value of WRMSD is equal to 1. A value of WRMSD close to 2 shows that the systematic and random errors are of the same order of magnitude. Results of the reduction of the VLE data are given in Table VI.

Vapor–liquid equilibrium data were independently fitted to the Wilson (*7*), NRTL (*8*), and modified UNIQUAC (*9*) equations. The model parameters were estimated by minimizing the ob-

Table VII. Parameters of Wilson, NRTL, and UNIQUAC Equation from VLE Data

		1-butanol (1)–methyl propanoate (2)			1-butanol (1)–methyl butanoate (2)		
model	T/K	parameters	100DP/P	100Dy	parameters	100DP/P	100Dy
Wilson	348.15	Λ_{12} = 0.6742 Λ_{21} = 0.7062	0.07	0.09	Λ_{12} = 0.6930 Λ_{21} = 0.6673	0.08	0.10
	368.19				Λ_{12} = 0.6895 Λ_{21} = 0.7792	0.11	0.22
NRTL	348.15	C_{12} = 103.80 C_{21} = 138.48 α = 0.1785	0.07	0.09	C_{12} = 137.91 C_{21} = 120.91 α = 0.3315	0.07	0.10
	368.19				C_{12} = 128.68 C_{21} = 140.59 α = 1.2302	0.06	0.16
UNIQUAC	348.15	A_{12} = 73.68 A_{21} = 215.79	0.08	0.09	A_{12} = 94.09 A_{21} = 206.77	0.08	0.10
	368.19				A_{12} = 43.78 A_{21} = 218.06	0.10	0.21

Table VIII. Temperature-Dependent NRTL Parameters Estimated from Vapor-Liquid Equilibrium and Heat of Mixing Data

model	system	parameters	data	100DP/P	100Dy	100Dh^E/h^E
NRTL	1-butanol (1)–methyl butanoate (2)	C_{12} = 145.50 + 0.3170(T − 273.15)	VLE(348.15)	0.50	0.18	
		C_{21} = 119.98 − 1.3852(T − 273.15)	VLE(368.19)	0.20	0.14	
		α = 0.0389 − 0.0312(T − 273.15)	h^E(298.15)			1.48

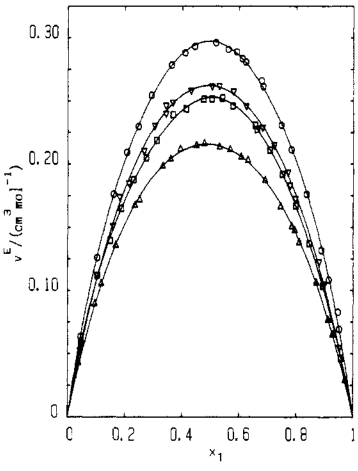

Figure 1. Excess molar volumes. Experimental results: (△) 1-butanol (1)–methyl butanoate (2) at 298.15 K; (□) 1-pentanol (1)–methyl butanoate (2) at 298.15 K; (▽) 1-butanol (1)–methyl propanoate (2) at 298.15 K; (○) 1-butanol (1)–methyl propanoate (2) at 308.15 K. The curves have been calculated from eq 1 with coefficients from Table III.

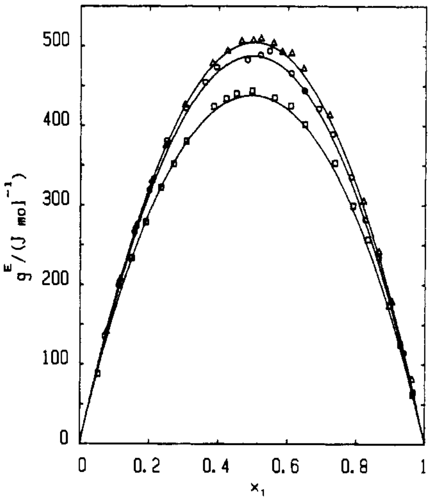

Figure 2. Excess Gibbs energies. Experimental results: (□) 1-butanol (1)–methyl butanoate (2) at 368.19 K; (○) 1-butanol (1)–methyl propanoate (2) at 348.15 K; (△) 1-butanol (1)–methyl butanoate (2) at 348.15 K. The curves have been calculated from eq 4 with coefficients from Table VI.

jective function S using the experimental inaccuracies $\sigma_e(p)$, $\sigma_e(T)$, and $\sigma_e(P)$ determined above. The parameters obtained are shown in Table VII together with the standard deviations given by

$$100(\mathrm{D}P/P) = (100/N)\sum_{i=1}^{N}|\Delta P_i|/P_i \qquad (6)$$

$$100\mathrm{D}y = (100/N)\sum_{i=1}^{N}|\Delta y_{1i}| \qquad (7)$$

Neau and Péneloux's successive reduction method (*10*) was used to fit the NRTL model to the combined vapor–liquid equilibrium data for one or more temperatures together with excess enthalpy data. Fernández et al. measured the excess enthalpies, h^E, at 298.15 K for both systems (*2*, *11*). The heat of mixing data were weighted assuming that experimental uncertainties are equal to $\sigma(h^E) = 0.01h^E$ in accordance with these experiments. The parameters of the models were assumed to vary linearly with temperature (see Appendix B). Table VIII shows the parameters obtained and the standard deviations on pressure, vapor composition (eq 6 and 7), and enthalpy which is given by

$$100(\mathrm{D}h^E/h^E) = (100/N)\sum_{i=1}^{N}|\Delta h^E|/h^E \qquad (8)$$

Discussion

The results of the reduction of our vapor–liquid equilibrium data show that they are thermodynamically consistent and that the estimated experimental inaccuracies are perfectly compatible with the calibration and characteristics of the apparatus. The Wilson, NRTL, and UNIQUAC models are all consistent with the experimental VLE data. The simultaneous reduction of the h^E and VLE data with the NRTL equation for the 1-butanol–methyl butanoate is satisfactory.

The obtained excess volumes are all positive and the corresponding curves are symmetric (see Figure 1). Analyzing the results for v^E obtained in the present paper with those of Fernández et al. (*3*) and Polak and Lu (*12*) we conclude that for both the methyl propanoate and the methyl butanoate mixtures at 298.15 K the excess volumes increase with the length of the alcohol chain. The same sequences has been obtained by Grolier and Viallard (*13*) for ethyl ethanoate–alcohol mixtures. These latter authors have given (*14*) an interpretation for this based on the predictions of the Barker theory.

Figure 2 shows that magnitude and symmetry of the excess Gibbs energy curves at 348.15 K are very similar for both systems studied. The g^E increases only slightly when we pass from the methyl propanoate to the methyl butanoate mixture (17 J mol^{-1} for $x_1 = 0.5$).

Appendix A

For N experimental measurements indicated by a superscript 0, the objective function used in the observed deviation method is given by

$$S = \sum_{i=1}^{N}[\Delta P_i/\sigma(P_i)]^2 + \sum_{i=1}^{N}(a_i \Delta P_i + b_i \Delta y_{1i})^2 \qquad \text{(A1)}$$

where

$$\Delta P = P^0 - P(x_1^0, A), \quad \Delta y_1 = y_1^0 - y_1(x_1^0, A)$$

$$a = -\delta P \delta y_1/\sigma(P) D^{1/2}, \quad b = \sigma(P)/D^{1/2} \qquad \text{(A2)}$$

$$D = \sigma^2(P)\,\sigma^2(y_1) - \overline{\delta P \delta y_1}^2$$

The corresponding variances and covariances are given by

$$\sigma^2(P) = \sigma_e^2(P) + (\partial P/\partial x_1)_T^2(\partial x_1/\partial \rho)_T^2\sigma_e^2(\rho) + (\partial P/\partial T)_{x_1}^2\sigma_e^2(T)$$

$$\sigma^2(y_1) = [(\partial y_1/\partial \rho)_T^2 + (\partial y_1/\partial x_1)_T^2(\partial x_1/\partial \rho)_T^2]\,\sigma_e^2(\rho) + (\partial y_1/\partial T)_{x_1}^2\sigma_e^2(T)$$

$$\delta P \delta y_1 = (\partial P/\partial x_1)_T(\partial y_1/\partial x_1)(\partial x_1/\partial \rho)_T\sigma_e^2(\rho) + (\partial P/\partial T)_{x_1}(\partial y_1/\partial T)_{x_1}\sigma_e^2(T) \qquad \text{(A3)}$$

Appendix B

The fundamental expressions of the Wilson, NRTL, and UNIQUAC models, whose parameters are listed in Tables VII and VIII, are as follows

WILSON

$$g^E/RT = -x_1 \ln(x_1 + \Lambda_{12}x_2) - x_2 \ln(x_2 + \Lambda_{21}x_1) \qquad \text{(B1)}$$

NRTL

$$g^E/(RTx_1x_2) = \frac{\tau_{21}G_{21}}{x_1 + x_2G_{21}} + \frac{\tau_{12}G_{12}}{G_{12}x_1 + x_2} \qquad \text{(B2)}$$

where

$$\tau_{kl} = C_{kl}/T \qquad G_{kl} = \exp(-\alpha\tau_{kl}) \qquad \text{(B3)}$$

$$C_{kl} = C_{kl}^C + C_{kl}^T(T - 273.15)$$

$$\alpha = \alpha^C + \alpha^T(T - 273.15)$$

UNIQUAC

$$g^E = g^E(\text{combinatorial}) + g^E(\text{residual}) \qquad \text{(B4)}$$

$$\frac{g^E(\text{combinatorial})}{RT} = x_1 \ln\frac{\phi_1}{x_1} + x_2 \ln\frac{\phi_2}{x_2} + \frac{z}{2}\left(q_1x_1 \ln\frac{\theta_1}{\phi_1} + q_2x_2 \ln\frac{\theta_2}{\phi_2}\right) \qquad \text{(B5)}$$

$$\frac{g^E(\text{residual})}{RT} = -q_1'x_1 \ln(\theta_1' + \theta_2'\tau_{21}) - q_2'x_2 \ln(\theta_2' + \theta_1'\tau_{12}) \qquad \text{(B6)}$$

where

$$\tau_{kl} = \exp\left(-\frac{A_{kl}}{T}\right) \qquad \text{(B7)}$$

$$\phi_1 = \frac{x_1r_1}{x_1r_1 + x_2r_2} \qquad \theta_1 = \frac{x_1q_1}{x_1q_1 + x_2q_2}$$

$$\theta_1' = \frac{x_1q_1'}{x_1'q_1' + x_2q_2'}$$

The parameters r_i, q_i, and q_i' are pure-component molecular-structure constants depending on molecular size and external surface areas. The parameters r_i and q_i have been determined by the method of Abrams and Prausnitz (*21*). For methyl propanoate and methyl butanoate we have used $q' = 1$ and for 1-butanol $q' = 0.85$.

Glossary

A_j	parameters of equation Redlich–Kister (v^E,g^E)
A_{ij}	parameter of UNIQUAC model
B_{ij}	second virial coefficients
C_{ij}	parameter of NRTL model
G_{ij}	parameter of NRTL model
h^E	excess molar enthalpy
m	number of Redlich–Kister parameters A_j
N	total number of measurements
P	total vapor pressure
P_i^s	vapor pressure of pure component i
S	objective function
T	temperature
v^E	excess molar volumes
v_i	liquid molar volume of pure component i
x_i	liquid mole fraction of component i
y_i	vapor mole fraction of component i

Greek Letters

α	parameter of NRTL model
γ_i	activity coefficient of component i
Λ_{ij}	parameter of Wilson model
ρ	density of a pure liquid or liquid mixture
σ_e	experimental uncertainty
σ	root of resulting variance

Superscripts

C	temperature-independent parameter
E	excess property
0	experimental value
1,2	molecular species (1 normally refers to alcohol, 2 to ester)
T	temperature-dependent parameter

Registry No. 1-Butanol, 71-36-3; methyl propanoate, 554-12-1; methyl butanoate, 623-42-7; 1-pentanol, 71-41-0.

Literature Cited

(1) Fernández, J.; Paz Andrade, M. I.; Sarmiento, F.; Bravo, R. *J. Chem. Thermodyn.* **1983**, *15*, 1145–1149.
(2) Fernández, J.; Berro, C.; Paz Andrade, M. I. *Fluid Phase Equilib.* **1985**, *20*, 145–153.
(3) Berro, C.; Rogalski, M.; Péneloux, A. *Fluid Phase Equilib.* **1982**, *8*, 55–73.
(4) Berro, C.; Péneloux, A. *J. Chem. Eng. Data* **1984**, *29*, 206–210.
(5) Hayden, J. G.; O'Connell, J. P. *Ind. Eng. Chem. Process Des. Dev.* **1975**, *14*, 209–216.
(6) Neau, E.; Péneloux, A. *Fluid Phase Equilib.* **1981**, *6*, 1–19.
(7) Wilson, G. M. *J. Am. Chem. Soc.* **1964**, *86*, 127–130.
(8) Renon, H.; Prausnitz, J. M. *AIChE J.* **1968**, *14*, 134–144.
(9) Anderson, T. F.; Prausnitz, J. M. *Ind. Eng. Chem. Process Des. Dev.* **1978**, *17*, 552–561.
(10) Neau, E.; Péneloux, A. *Fluid Phase Equilib.* **1982**, *8*, 251–269.
(11) Fernández, J.; Pintos, M.; Baluja, M. C.; Jiménez, E.; Paz Andrade, M. I. *J. Chem. Eng. Data* **1985**, *30*, 318–320.
(12) Polak, J.; Lu, B. C.-Y. *J. Chem. Eng. Data.* **1972**, *17*, 456–458.
(13) Grolier, J. P.; Viallard, A. *J. Chim. Phys.* **1971**, *68*, 1442–1448.
(14) Grolier, J.-P.; Viallard, A. *J. Chim. Phys.* **1972**, *69*, 202–211.

(15) Hales, J. L.; Ellender, J. H. *J. Chem. Thermodyn.* **1976**, *8*, 1177-1184.
(16) Dusart, O.; Piekarski, C.; Piekarski, S.; Viallard, A. *J. Chim. Phys.* **1976**, *73*, 837-844.
(17) Ambrose, D.; Sprake, C. H. S. *J. Chem. Thermodyn.* **1970**, *2*, 631-645.
(18) Reid, R. C.; Prausnitz, J. M.; Sherwood, T. K. *The Properties of Gases and Liquids*, 3rd ed.; McGraw-Hill: New York, 1977.
(19) Mertl, I.; Polak, J. *Collect. Czech. Chem. Commun.* **1965**, *30*, 3526-3528.
(20) Wisniak, J.; Tamir, A. *J. Chem. Eng. Data* **1964**, *29*, 19-20.
(21) Abrams, D. J.; Prausnitz, J. M. *AIChE J.* **1975**, *21*, 116-128.

Received for review October 8, 1985. Accepted July 7, 1986.

Solubility of Hydrogen in Alcohols and Esters

Mark S. Wainwright,* Thomas Ahn, and David L. Trimm

School of Chemical Engineering and Industrial Chemistry, The University of New South Wales, Kensington, New South Wales, 2033 Australia

Noel W. Cant

School of Chemistry, Macquarie University, North Ryde, New South Wales, 2113 Australia

The solubility of hydrogen in various alcohols and esters has been measured at pressures up to ca. 5 MPa by gas chromatographic analysis of equilibrated gas-in-liquid mixtures from a stirred autoclave vessel. Typical dilute solution behavior was observed, and the Henry's law coefficients for hydrogen solubility in normal alcohols and corresponding esters at 291 K are presented. A batch gas absorption technique based on pressure and volume measurements was shown to significantly underestimate solubility when values of hydrogen solubility in methyl alcohol and methyl formate were compared with those obtained by analysis of the gas dissolved in the liquid phase.

Introduction

There has recently been considerable interest in the liquid-phase synthesis of methanol (*1*). This process involves the carbonylation of the alcohol

$$ROH + CO \rightarrow HCOOR \qquad (1)$$

to produce a formate ester, and a simultaneous or sequential hydrogenolysis step to produce the parent alcohol and a molecule of methanol. This hydrogenolysis, which is conducted as a slurry phase reaction at pressures up to 10 MPa (*1*, *2*), can be represented as

$$HCOOR + 2H_2 \rightarrow ROH + CH_3OH \qquad (2)$$

Reactions conducted by using this form of contacting are frequently limited by mass-transfer considerations and it is therefore essential to have some knowledge of the solubility of the reacting gases in the liquid reactants and products. In a recent study (*3*) we presented CO solubility data for a wide range of alcohols. A review of the literature reveals that studies of H_2 solubility in lower alcohols have been made for methanol (*4*-*9*), ethanol (*4*, *9*), 1-propanol (*4*, *9*, *10*), and 1-butanol (5, 9-11). Measurements for corresponding esters have been limited to methyl acetate (*9*, *12*) and ethyl acetate (*9*, *13*, *14*). Many of those investigations were restricted to pressures less than 0.2 MPa. The present study was therefore undertaken to provide solubility data at pressures up to around 5 MPa on alcohols and esters that have been studied in hydrogenolysis reactions in this laboratory.

Experimental Section

The measurements were carried out in the apparatus used in the earlier study of CO solubility (*8*). It consisted of a 300-cm^3 stirred autoclave (Autoclave Engineers, PA) which was rated to 34 MPa. The experiments were conducted in a constant temperature room at 291 K. The temperature of the liquid in the autoclave was measured with a calibrated 1 mm o.d., stainless-steel sheathed, chromel-alumel thermocouple, the output of which was continuously monitored by using a digital voltmeter. The temperature of the liquid in the autoclave was 291 ± 1 K for all experiments. The pressure was measured to within ±10 kPa with a standardized Bourdon-type gauge. More complete details and a diagram of the apparatus are presented elsewhere (*3*).

Solubility measurements were carried out by initially placing 200 cm^3 of the solvent of interest in the autoclave and pressurizing the system to the desired level (1-5 MPa) from a cylinder of hydrogen. After stirring for 10 min to achieve equilibration, a sample of the liquid phase was taken for analysis by drawing a fine stream from the autoclave through a four-port Valco HPLC valve. The valve which had an internal loop volume of 1.0 μL was maintained at the same temperature as the autoclave (291 K). The flow was then shut off after the valve, and after about 30 s was allowed for pressure equilibration between the valve and the autoclave, the 1-μL sample was switched into a stream of high-purity nitrogen carrier gas (25 $cm^3\ min^{-1}$) where it vaporized and was carried to a Gow-Mac gas chromatograph fitted with a thermal conductivity detector. A 1.8-m column of Porapak N, maintained at 378 K, was used to separate the hydrogen peak from the peak(s) of the liquid-phase components. Peak integration was achieved with a Hewlett Packard 3390 A reporting integrator. Replicated measurements at longer times revealed no increase in the area of the hydrogen peak, indicating that equilibrium absorption was obtained in 10 min. Calibration was achieved by determining the peak areas corresponding to known pressures of hydrogen gas alone in the loop. The plot of peak area vs. hydrogen pressure was highly linear as expected for small quantities of hydrogen in nitrogen carrier gas. Calibrations by injecting pure H_2 at pressure P_c were performed before and after solubility

0021-9568/87/1732-0022$01.50/0